

# Evidence of many-body localization in 2D from quantum Monte Carlo simulation

Ho-Kin Tang,<sup>1,2</sup> N. Swain,<sup>1,3</sup> D. C. W. Foo,<sup>1</sup> B. J. J. Khor,<sup>1</sup> F. F. Assaad,<sup>4</sup> S. Adam,<sup>5,6,7,1</sup> and P. Sengupta<sup>1,3</sup>

<sup>1</sup>Centre for Advanced 2D Materials, National University of Singapore, 6 Science Drive 2, Singapore 117546

<sup>2</sup>Shenzhen JL Computational Science and Applied Research Institute, Shenzhen 518109, China

<sup>3</sup>School of Physical and Mathematical Sciences, Nanyang Technological University, 21 Nanyang Link, Singapore 637371

<sup>4</sup>Institut für Theoretische Physik und Astrophysik and Würzburg-Dresden Cluster of Excellence ct.qmat, Universität Würzburg, 97074 Würzburg, Germany

<sup>5</sup>Department of Materials Science and Engineering,

National University of Singapore, 9 Engineering Drive 1, Singapore 117575

<sup>6</sup>Yale-NUS College, 16 College Ave West, Singapore 138527

<sup>7</sup>Department of Physics, Faculty of Science, National University of Singapore, 2 Science Drive 3, Singapore 117542

(Dated: June 17, 2021)

We use the stochastic series expansion quantum Monte Carlo method, together with the eigenstate-to-Hamiltonian mapping approach, to map the localized ground states of the disordered two-dimensional Heisenberg model, to excited states of a target Hamiltonian. The localized nature of the ground state is established by studying the spin stiffness, local entanglement entropy, and local magnetization. This construction allows us to define many body localized states in an energy resolved phase diagram thereby providing concrete numerical evidence for the existence of a many-body localized phase in two dimensions.

*Introduction:* Disorder and interactions induce novel phases and phenomena in quantum many body systems. Anderson showed that for non-interacting systems in one and two dimensions, *all* single particle eigenstates are localized in the presence of disorder [1, 2]. In recent years, it has emerged that localization of the entire eigenspectrum persists in the presence of interactions and strong disorder, constituting Many Body Localization (MBL) – a phenomenon that has been subject to intense investigation since its inception due to both fundamental and practical reasons [3, 4]. The MBL phase is a new phase of matter that breaks ergodicity and violates the Eigenvalue Thermalization Hypothesis (ETH) [4–6]. In this phase, a closed system does not thermalize under its own dynamics, and hence cannot be described within the framework of conventional quantum statistical physics. At the same time, the long memory associated with the slow dynamics makes the MBL phase appealing for many practical applications [7–9].

The existence of the MBL phase in one dimension has been well established through numerical [10–13] and analytical studies [14] as well as in experiments [15, 16]. On the other hand, its fate in two dimensions has been contentious, though evidence is accumulating towards the affirmative [17, 18]. In this work, as shown in Fig. 1, we present convincing numerical evidence for the existence of MBL states in the 2D Heisenberg antiferromagnet. Using the Eigenstate-to-Hamiltonian construction (EHC) approach described in [19–21], we map the Bose Glass (BG) ground state obtained from large scale quantum Monte Carlo (QMC) simulations of the 2D Heisenberg antiferromagnet with random onsite disorder to an excited state of another Hamiltonian that differs only in terms of the distribution and magnitude of the random fields. This allows us to identify the mobility edge separating the delocalized and MBL regimes in 2D spin systems [22].

*Background:* Establishing the existence of MBL in 2D is significantly more challenging than in 1D. From a computational perspective, exact diagonalization (ED) is limited to system sizes that are too small to provide any meaningful energy level statistics. Hence extending 1D methods to 2D suffers from inherent bias. Local integrals of motion (LIOM) – a defining characteristic of MBL in 1D – are not exact in 2D, making their use in proving the existence of MBL in 2D less reliable. Tensor network approaches in 2D are not as efficient as their 1D counterparts, because higher dimensionality introduces effective long-range interactions in the product state construction.

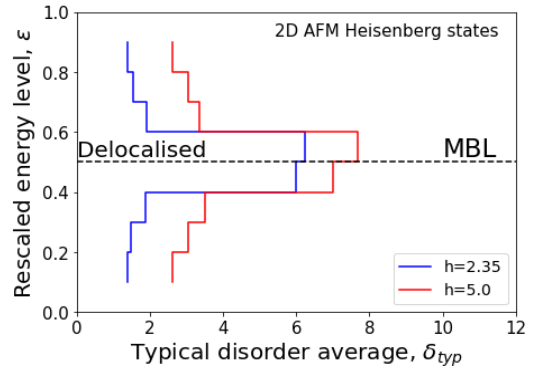


FIG. 1. The delocalized (see text) to MBL phase boundary in the eigenspectrum vs typical disorder phase diagram is calculated using the eigenstate-to-hamiltonian construction, with the ground state eigenstate determined by large-scale unbiased quantum Monte Carlo simulations. We show the mapping of localized ground states with 3000 random disorder realizations with maximum strength  $h = 2.35$  and  $h = 5.0$  on a  $16 \times 16$  square lattice. The mobility edge corresponds to the phase boundary obtained with the critical disorder strength ( $h_c \approx 2.35$ ) for the localization transition in the ground state.

Finally, it is difficult to differentiate between slow exponential versus algebraic decay in finite time simulations. Hence there is an urgent need for unbiased and complementary computational approaches such as quantum Monte Carlo methods to conclusively determine the existence of MBL in 2D disordered systems.

On the other hand, there have been persistent controversy questioning the existence of MBL as a thermodynamic phase, although there is a growing consensus towards an affirmative answer. Non-convergence of perturbation theory about the non-interacting phase for certain types of arbitrarily weak disorder was presented as evidence for the non-existence of MBL [23], though the argument is now understood as stating that any putative MBL state is not connected to the non-interacting phase, not that the MBL state itself does not exist. Other work suggested that rare regions of low local disorder may form ergodic bubbles that precipitate an avalanche effect, completely thermalising the MBL phase [24], however later works have identified circumstances under which such avalanche events do not occur, or are not observable in an experimentally accessible timeframe, allowing for the conclusion that the avalanche mechanism is not nearly as universal as first proposed [25]. Argument concerning whether the ETH-MBL transition is truly a transition or merely a crossover, and that the apparent transition seen in numerical studies is merely a finite size effect [25, 26] are gravely weakened by the fact that exactly solvable systems in which MBL is known to exist also exhibit the same finite size effects and scaling behaviour [27]. The possibility remains open then that for 2D studies, such finite size effects may not be relevant, nonetheless we remain vigilant against such hasty conclusions.

In contrast, experiments in cold atomic fermion and boson systems have consistently provided positive signatures of MBL phase in 1D and higher dimensions [15, 28, 29]. Relaxation dynamics of interacting  $^{40}\text{K}$  atoms in a 2D optical lattice with quasiperiodic potential have demonstrated complete suppression of relaxation beyond a critical disorder strength on experimentally accessible time scales, providing strong evidence of MBL phase in 2D [30]. While questions still persist on the occurrence of rare ergodic regions near the transition boundary leading to a thermal avalanche and destabilisation of the MBL phase [31, 32], a recent study shows that such an avalanche scenario can be avoided under realistic conditions, adding further confirmation of the occurrence of MBL transition in 2D [33].

A different line of study has emerged in recent years wherein one considers the ground state of interacting bosons or fermions with disorder (for which powerful numerical techniques exist in 2D and 3D) and then uses an Eigenstate to Hamiltonian Construction (EHC) formalism to identify Hamiltonians for which the said ground state is an excited state. This was used in Ref.[21, 34] to obtain the mobility edge of the 1D disordered Heisenberg model. Although the MBL is a property of the excited states, it shares several features in common with

the ground state of disordered bosons; in particular, they both obey an area law for the entanglement entropy. The interplay between strong interactions and disorder in the *ground state* of interacting bosons has been extensively studied and results in the well-known BG phase. For 1D disordered spin systems, it was recently shown that an MBL state of any particular Hamiltonian corresponds to the BG ground state of another Hamiltonian of the same form [21, 34], but with different local disorder distribution. This provides a powerful, controlled numerical approach to determining Hamiltonians with MBL eigenspectrum through the EHC framework. In this work, we generalise the EHC approach to establish MBL in the two dimensional Heisenberg model with random site disorder using unbiased QMC simulations to evaluate the ground state of the parent Hamiltonian.

*Model:* The 2D spin-1/2 Heisenberg model with random magnetic fields is described by the Hamiltonian,

$$\mathcal{H} = J \sum_{\langle i,j \rangle} \mathbf{S}_i \cdot \mathbf{S}_j + \sum_i h_i S_i^z \quad (1)$$

where  $\mathbf{S}_i$  is the spin operator at site  $i$ ,  $\langle i,j \rangle$  indicates a sum over nearest-neighbour sites, and  $h_i \in [-h, h]$  represents the local random magnetic field disorder. We shall consider antiferromagnetic exchange interaction ( $J > 0$ ) and set  $J = 1$  as the energy scale. The Hamiltonian commutes with the total magnetization,  $S_{\text{tot}}^z = \sum_i S_i^z$ , and only states in the  $S_{\text{tot}}^z = 0$  sector are considered while evaluating the ground state.

*Method:* We begin by finding the localized BG ground state  $|\Psi_0\rangle$  of a particular parent Hamiltonian  $\mathcal{H}$  of the form Eqn. (1) using the stochastic series expansion (SSE) QMC method [35–37], which has been successfully used

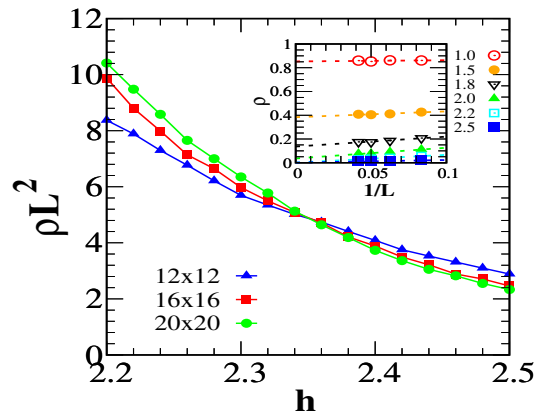


FIG. 2. (Main) Behaviour of the scaled stiffness,  $L^2 \rho_s$ , with varying  $h$  near the transition region. The curves for different system sizes cross at  $h = h_c$ , providing an accurate estimate of the critical disorder strength,  $h_c \approx 2.35$ . (Inset) Finite size scaling of the spin stiffness,  $\rho$ , with varying system sizes for different disorder strengths. It can be seen that in the thermodynamic limit  $\rho = 0$ , as  $h \geq h_c$ , establishing the BG phase as the ground state.

in the past to probe the BG transition [38–41]. The localized ground state is identified by calculating the spin stiffness, local magnetization, and local entanglement entropy.

Next we conduct a search for a new Hamiltonian,  $\tilde{\mathcal{H}}$ , with the same form as  $\mathcal{H}$  as in Eqn. (1), but different random field distribution, for which  $|\Psi_0\rangle$  as an eigenstate [19, 20]. The target Hamiltonian,  $\tilde{\mathcal{H}}$ , is obtained by analyzing the quantum covariance matrix (QCM) defined in terms of the ground state expectation values of the local Hamiltonian operators of  $\mathcal{H}$  as

$$C_{ij} = \langle \mathcal{O}_i \mathcal{O}_j \rangle - \langle \mathcal{O}_i \rangle \langle \mathcal{O}_j \rangle, \quad (2)$$

where  $\mathcal{O}_0 = \sum_{\langle i,j \rangle} S_i^z S_j^z$  and  $\mathcal{O}_i = S_i^z$ ,  $i = 1, \dots, N$ . The eigenvectors of the QCM contain the parameters  $\{\tilde{J}, \tilde{h}_1, \dots, \tilde{h}_N\}$  defining a target Hamiltonian,  $\tilde{\mathcal{H}}$ , and the corresponding eigenvalue gives the variance of the energy of  $|\Psi_0\rangle$  with respect to  $\mathcal{H}$ . A vanishing eigenvalue of QCM signals that  $|\Psi_0\rangle$  is an eigenstate of  $\tilde{\mathcal{H}}$  with energy  $E = \langle \Psi_0 | \tilde{\mathcal{H}} | \Psi_0 \rangle$ . We search for zero eigenvalues of the QCM in order to determine the target Hamiltonians. In contrast to ED and DMRG algorithms, QMC simulations do not yield the ground state wavefunction so  $E$  cannot be evaluated directly. Instead, it is estimated by storing the components of the energy of  $|\Psi_0\rangle$  in  $\mathcal{H}$  and rescaling them by the parameters of  $\tilde{\mathcal{H}}$  [42]. To compare eigenvalues of  $|\Psi_0\rangle$  in different  $\tilde{\mathcal{H}}$ , we introduce the rescaled energy level,  $\epsilon = (E - E_{\min}) / (E_{\max} - E_{\min})$ , where  $E_{\min}$  and  $E_{\max}$  are the minimum and maximum eigenvalues of  $\tilde{\mathcal{H}}$  that are determined from independent QMC simulations of  $\tilde{\mathcal{H}}$  and  $-\tilde{\mathcal{H}}$  respectively. Working with an ordered set of eigenvalues,  $e_0, e_1, \dots, e_N$ , of the QCM, we note that the first two eigenvalues,  $e_0$  and  $e_1$  are always zero (up to numerical precision) - these correspond to the parent Hamiltonian,  $\mathcal{H}$  and the constraint  $S_{\text{tot}}^z = 0$ . Any other vanishing eigenvalues will correspond to a new target Hamiltonian [19]. Successfully identifying Hamiltonians of the same form whose excited states are identical to localized ground states of  $\mathcal{H}$  provides conclusive numerical evidence of the presence of MBL in two dimensional spin systems. A key advantages of the EHC is that it is complete, in the sense that if and only if the target Hamiltonian space contains a particular (set of) Hamiltonian(s) satisfying the specified search criteria, it will indeed be found [19]. This ensures that the mapping of eigenstates is complete and allows us to accurately pin down the mobility edge.

The measurement of the covariance matrix requires new measuring techniques in the stochastic series expansion approach. Details of this implementation can be found in the Supplementary Material. Following its evaluation, we diagonalize the covariance matrix and focus on  $e_3$  - which is typically small in magnitude, but not zero due to numerical precision - and its finite-size dependence to verify whether  $|\Psi_0\rangle$  is an eigenstate of the Hamiltonian represented by the corresponding eigenvector. The associated eigenvector gives the parameters of

the new Hamiltonian  $\tilde{\mathcal{H}}(\tilde{J}, \tilde{h}_1, \dots, \tilde{h}_N)$ . The eigenvalues decay algebraically with lattice size (see Fig. 3), ensuring the accuracy of the mapping [19]. The eigenvalues here are energy variances and so the algebraic decay with system size is consistent with the exponential decay of gaps in the Hamiltonian spectrum. Furthermore, the decay of the energy variance ensures that the MBL state energy is self-averaging.

*Results:* In the presence of uniformly distributed random disorder,  $h_i \in [-h, h]$ , the transition to a localized ground state (Bose glass) for the AFM Heisenberg model in 2D occurs at a non-zero critical field,  $h = h_c$  [41]. For  $h > h_c$ , the localized ground state can be mapped to MBL (excited) states of Hamiltonians that differ in the random local fields. The critical disorder strength,  $h_c$ , can be determined from the scaling of the ground state spin stiffness,  $\rho$ , defined as the response of the total energy to a twist,  $\rho_s = \frac{1}{N} \frac{\partial^2 E}{\partial \phi^2}$ . In SSE, the stiffness is measured by the fluctuation in winding number ( $W$ ) of the world lines as  $\rho_s = \langle W^2 \rangle / 2\beta$ , where  $\beta$  is the inverse temperature ( $\beta = 8L$  in our simulations ensures the study in the ground state). Close to the critical point, the stiffness obeys the scaling form

$$\rho_s(L, h) = L^{-z} f[(h - h_c)L^{1/\nu}], \quad (3)$$

where the correlation length exponent is  $\nu = 1$  [40], and the dynamical critical exponent is found to be  $z = 2$ . Plotting the scaled stiffness  $L^z \rho_s$  against  $h$  for different system sizes provides an accurate estimate of the critical disorder strength,  $h_c$  [41]. The results are shown in fig.(2), which suggest  $h_c \approx 2.35$ . The interacting ground state changes from a delocalized superfluid state to a lo-

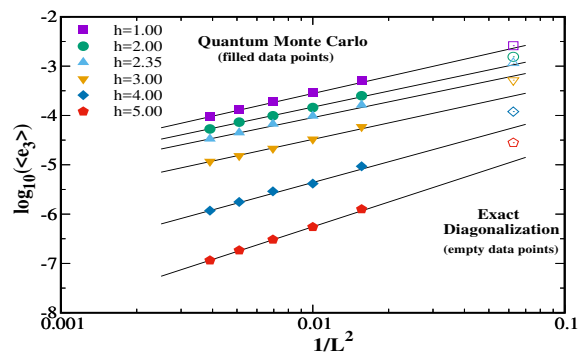


FIG. 3. Finite size scaling of the third eigenvalue,  $e_3$  of the QCM with varying system sizes ( $L \times L$ ). The filled data points refer to the data from quantum Monte Carlo (QMC) simulation, whereas the empty data points refer to the data from exact diagonalisation (ED) calculation. From the ground state of the parent Hamiltonian  $\mathcal{H}$  with the magnetic disorder magnitude  $h$ , we calculate the quantum covariance matrix and find  $e_3$ . The corresponding eigenvector is used to obtain the new Hamiltonian  $\tilde{\mathcal{H}}$ .  $e_3$  average is taken over 1000 independent disorder realizations of different disorder strengths  $h$ . Our results suggest an algebraic decay of  $e_3$  against the lattice size  $L^2$  for different  $h$ .

calized Bose glass state for  $h > h_c$ . We use the ground state as the input state in the EHC approach. As a result the ground states of our target Hamiltonian carries two groups of distinguishable properties, the delocalized state with  $h < h_c$  and the localized state with  $h > h_c$ .

To search for the existence of MBL in 2D, we investigate whether the Bose glass ground state of  $\mathcal{H}$  for any disorder realization ( $h > h_c$ ) can be mapped to an excited state of a new Hamiltonian by the EHC scheme discussed above. We start by constructing and then diagonalizing the quantum covariance matrix, looking for eigenstates with zero eigenvalue. As stated earlier,  $e_0$  and  $e_1$  are both zero as they correspond to the parent Hamiltonian and the conserved total magnetization. Instead, we focus on the next smallest positive eigenvalue  $e_3$ . We find that  $e_3$  vanishes in the thermodynamic limit, implying that  $|\Psi_0\rangle$  is an excited eigenstate of a Hamiltonian parametrized by the corresponding eigenvector. From this, following [21], we calculate the typical disorder average  $\delta_{typ} = \exp(\langle \ln(|\tilde{h}_i - \tilde{h}_{i+1}|) \rangle)$ , which measures the degree of disorders in the new disorder distribution [43].

For each disorder realization in  $\mathcal{H}$ , we obtain the parent ground state  $|\psi\rangle$  and the new Hamiltonian  $\tilde{\mathcal{H}}$  by the eigenstate-to-Hamiltonian approach; we find the energy of the excited state  $E = \langle \Psi_0 | \tilde{H} | \Psi_0 \rangle$ . Through simulation of  $\tilde{\mathcal{H}}$  and  $-\tilde{\mathcal{H}}$ , we calculate the corresponding ground state energies  $E_{min}$  and  $-E_{max}$  respectively. We rescale the energy of the excited state in  $\tilde{H}$  as  $\epsilon = (E - E_{min}) / (E_{max} - E_{min})$ , such that,  $\epsilon \in [0, 1]$  corresponds to the full eigenspectrum of the many-body Hamiltonian. In total, we simulate over 3000 disorder realizations for different disorder strengths. Using the typical average of the mapped disorder  $\tilde{h}$ , we obtain the energy-resolved phase diagram, with the energy  $\epsilon \in [0, 1]$  (see fig.1).

Our main finding of the MBL phase transition is shown in Fig. 1. It is clearly seen that the strength of the new disorder,  $\tilde{h}$ , is larger than the original disorder strength,  $h$  (see Supplementary Material). We have verified the EHC formalism works in the delocalized regime. The mapped states also violate ETH, but are delocalized. As our focus is in the localized regime, we will not discuss them in detail here. Further for strong enough disorder strength, the excited states are identical to the localized ground state. The dependence of  $\epsilon$  with  $\delta_{typ}$  gives an indication of the mobility edge in our study.

We further investigate some physical properties of the ground state of the parent Hamiltonian, as it is shared with the mapped excited states of the new Hamiltonian. In Fig. 4, we show the distribution of local magnetization for representative values of disorder strengths corresponding to the delocalized ( $h = 1$ ) and localized ( $h = 5$ ) phases. We find a sharp feature of bipolar local magnetization (with values  $+1/2$  and  $-1/2$ ) appearing when the system is in the localized phase ( $h = 5$ ), while the delocalized phase ( $h = 1$ ) shows uniformly distributed magnetization values centered around zero.

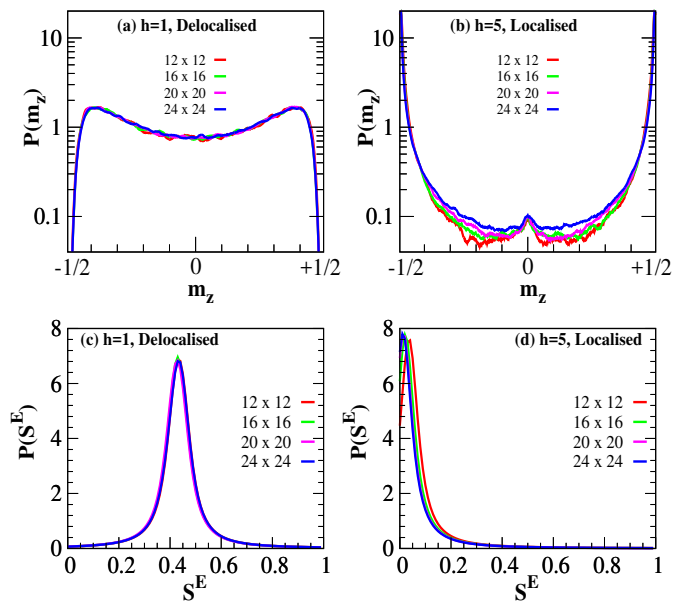


FIG. 4. (Top panel) Distribution of local magnetisation  $P(m_z)$  in the ground state for different system sizes and disorder strength (a)  $h = 1$  and (b)  $h = 5$  showing two distinct behaviors.  $m_z$  is averaged over 1000 disorder realizations. For  $h = 1$ ,  $m_z$  fluctuates strongly between  $[-h, h]$ , however, this fluctuation is strongly suppressed for  $h = 5$ .  $P(m_z = 0)$  reduces with increasing disorder strength. (Bottom panel) Distribution of local (on-site) entanglement entropy  $P(S^E)$  in the ground state for disorder strength  $h = 1$  (a) and  $h = 5$  (b).  $P(S^E)$  is averaged over 1000 disorder realisations.  $P(S^E)$  shows a maximum at  $S^E \neq 0$  for  $h = 1$  signifying a site is strongly entangled with its neighboring sites (characteristic of delocalized phase), whereas it shows a sharp peak at  $S^E \sim 0$  for  $h = 5$  indicating that a site gets disentangled from its neighboring sites (characteristic of localized phase). The  $S^E$  peak moves to  $S^E = 0$  with increasing system sizes.

Further, we measure the local entanglement entropy  $S^E = -\ln \rho_{loc}^2$  using the extended ensemble scheme [44–46] within the SSE approach. In Fig. 4, we compare the behavior of the local entanglement entropy in the localized and delocalized phases by calculating their distribution,  $P(S^E)$ . In the localized phase ( $h = 5$ ),  $P(S^E)$  shows a sharp peak at  $S^E = 0$ . This is a prominent feature of localization, where any given site is disentangled from other sites of the lattice. The eigenstate can be transformed to a product state by a sequence of quasi-local unitary transformation [47]. On the other hand, in the delocalized phase ( $h = 1$ ),  $P(S^E)$  displays a continuous distribution with a sharp peak like feature for  $S^E \approx 1/2$ . No  $S^E = 0$  peak is observed in  $P(S^E)$ . The eigenstate is entangled in this regime. Our results show convergence of the data with different system sizes.

*Conclusions:* In summary, we have presented conclusive numerical evidence of the existence of many-body localized states, which violate ETH in the two dimensional Heisenberg model with magnetic disorders. We use unbiased QMC simulation to calculate the local-

ized (Bose glass) ground state of the antiferromagnetic Heisenberg model with random site disorder. Our results show that there is a transition to the Bose glass phase in the ground state at disorder strength  $h_c \approx 2.35J$ . For disorder strength  $h > h_c$ , the localized ground state can be mapped to the excited state of a different Hamiltonian through the Eigenstate to Hamiltonian mapping. The disorder distribution of the new Hamiltonian is obtained from analyzing the quantum covariance matrix of the parent Hamiltonian. Our results provide concrete evidence for the existence of the many-body localized phase in a system with dimensionality higher than one. The mapped excited states at the phase transition boundary is identified as the mobility edge. During the preparation of this manuscript, we found a similar study using 1-bits to study the many-body localization transition in 2- and 3-dimensional systems [18].

## ACKNOWLEDGMENTS

H.-K. Tang and N. Swain contributed equally to this work. We thank Gabriel Lemarie, Maxime Dupont and Rubem Mondaini for helpful discussions, and Miguel Dias Costa for assistance with the numerical parallelization of our code. This work is supported by the Singapore Ministry of Education AcRF Tier 2 grant (MOE2017-T2-1-130), and made possible by allocation of computational resources at the Centre for Advanced 2D Materials (CA2DM), and the Singapore National Super Computing Centre (NSCC). FFA thanks support from the Würzburg-Dresden Cluster of Excellence on Complexity and Topology in Quantum Matter ct.qmat (EXC 2147, project-id 390858490).

- 
- [1] P. W. Anderson, *Phys. Rev.* **109**, 1492 (1958).  
 [2] F. Evers and A. D. Mirlin, *Rev. Mod. Phys.* **80**, 1355 (2008).  
 [3] D. Basko, I. Aleiner, and B. Altshuler, *Ann. Phys. (N. Y.)* **321**, 1126 (2006).  
 [4] R. Nandkishore and D. A. Huse, *Annu. Rev. Condens. Matter Phys.* **6**, 15 (2015).  
 [5] F. Alet and N. Laflorencie, *C. R. Phys.* **19**, 498 (2018).  
 [6] D. A. Abanin, E. Altman, I. Bloch, and M. Serbyn, *Rev. Mod. Phys.* **91**, 021001 (2019).  
 [7] D. A. Huse, R. Nandkishore, V. Oganesyan, A. Pal, and S. L. Sondhi, *Phys. Rev. B* **88**, 014206 (2013).  
 [8] D. Pekker, G. Refael, E. Altman, E. Demler, and V. Oganesyan, *Phys. Rev. X* **4**, 011052 (2014).  
 [9] Y. Bahri, R. Vosk, E. Altman, and A. Vishwanath, *Nat. Commun.* **6**, 1 (2015), 1307.4092.  
 [10] D. J. Luitz, N. Laflorencie, and F. Alet, *Phys. Rev. B* **91**, 1 (2015), arXiv:1411.0660.  
 [11] M. Serbyn and J. E. Moore, *Phys. Rev. B* **93**, 1 (2016), arXiv:1508.07293.  
 [12] V. Khemani, F. Pollmann, and S. L. Sondhi, *Phys. Rev. Lett.* **116**, 1 (2016).  
 [13] S. P. Lim and D. N. Sheng, *Phys. Rev. B* **94**, 1 (2016).  
 [14] J. Z. Imbrie, V. Ros, and A. Scardicchio, *Annalen der Physik* **529**, 1 (2017).  
 [15] M. Schreiber, S. S. Hodgman, P. Bordia, H. P. Lüschen, M. H. Fischer, R. Vosk, E. Altman, U. Schneider, and I. Bloch, *Science* **349**, 842 (2015).  
 [16] J. Smith, A. Lee, P. Richerme, B. Neyenhuis, P. W. Hess, P. Hauke, M. Heyl, D. A. Huse, and C. Monroe, *Nat. Phys.* **12**, 907 (2016).  
 [17] T. B. Wahl, A. Pal, and S. H. Simon, *Nat. Phys.* **15**, 164 (2019).  
 [18] E. Chertkov, B. Villalonga, and B. K. Clark, *Phys. Rev. Lett.* **126**, 180602 (2021).  
 [19] E. Chertkov and B. K. Clark, *Phys. Rev. X* **8**, 031029 (2018).  
 [20] X. L. Qi and D. Ranard, *Quantum* **3**, 159 (2019).  
 [21] M. Dupont and N. Laflorencie, *Phys. Rev. B* **99**, 020202 (2019).  
 [22] By construction, our states satisfy an area law for the entanglement entropy such that the ETH is violated even in the delocalized phase.  
 [23] R. Nandkishore, *Phys. Rev. B* **90**, 184204 (2014).  
 [24] W. De Roeck and F. Huveneers, *Phys. Rev. B* **95**, 155129 (2017).  
 [25] I. D. Potirniche, S. Banerjee, and E. Altman, *Phys. Rev. B* **99**, 205149 (2019).  
 [26] J. Šuntajs, J. Bonča, T. c. v. Prosen, and L. Vidmar, *Phys. Rev. E* **102**, 062144 (2020).  
 [27] D. Abanin, J. Bardarson, G. De Tomasi, S. Gopalakrishnan, V. Khemani, S. Parameswaran, F. Pollmann, A. Potter, M. Serbyn, and R. Vasseur, *Ann. Phys. (N. Y.)* **427**, 168415 (2021).  
 [28] J. Y. Choi, S. Hild, J. Zeiher, P. Schauß, A. Rubio-Abadal, T. Yefsah, V. Khemani, D. A. Huse, I. Bloch, and C. Gross, *Science* **352**, 1547 (2016).  
 [29] S. S. Kondov, W. R. McGehee, W. Xu, and B. DeMarco, *Phys. Rev. Lett.* **114**, 083002 (2015).  
 [30] P. Bordia, H. P. Lüschen, S. S. Hodgman, M. Schreiber, I. Bloch, and U. Schneider, *Phys. Rev. Lett.* **116**, 140401 (2016).  
 [31] P. Bordia, H. Lüschen, S. Scherg, S. Gopalakrishnan, M. Knap, U. Schneider, and I. Bloch, *Phys. Rev. X* **7**, 041047 (2017).  
 [32] A. Rubio-Abadal, J.-y. Choi, J. Zeiher, S. Hollerith, J. Rui, I. Bloch, and C. Gross, *Phys. Rev. X* **9**, 041014 (2019).  
 [33] M. Sbroscia, K. Viebahn, E. Carter, J.-C. Yu, A. Gaunt, and U. Schneider, *Phys. Rev. Lett.* **125**, 200604 (2020).  
 [34] M. Dupont, N. Macé, and N. Laflorencie, *Phys. Rev. B* **100**, 134201 (2019).  
 [35] A. W. Sandvik, *J. Phys. A: Math. Gen.* **25**, 3667 (1992).  
 [36] A. W. Sandvik, *Phys. Rev. B* **59**, R14157 (1999).  
 [37] P. Sengupta and S. Haas, *Phys. Rev. Lett.* **99**, 050403 (2007).  
 [38] M. P. Fisher, P. B. Weichman, G. Grinstein, and D. S. Fisher, *Phys. Rev. B* **40**, 546 (1989).  
 [39] L. Pollet, N. V. Prokof'ev, B. V. Svistunov, and M. Troyer, *Phys. Rev. Lett.* **103**, 140402 (2009).  
 [40] N. Prokof'ev and B. Svistunov, *Phys. Rev. Lett.* **92**, 015703 (2004).

- [41] J. P. Álvarez Zúñiga, D. J. Luitz, G. Lemarié, and N. Laflorencie, [Phys. Rev. Lett. \*\*114\*\*, 155301 \(2015\)](#).
- [42] A. Sandvik and R. Singh, [Phys. Rev. B \*\*56\*\*, 14510 \(1997\)](#).
- [43] A remarkable property of the mapping is the emergence correlations in  $\tilde{h}_i$ .
- [44] S. Humeniuk and T. Roscilde, [Phys. Rev. B \*\*86\*\*, 235116 \(2012\)](#).
- [45] D. J. Luitz, X. Plat, N. Laflorencie, and F. Alet, [Phys. Rev. B \*\*90\*\*, 125105 \(2014\)](#).
- [46] D. J. Luitz, F. Alet, and N. Laflorencie, [Phys. Rev. Lett. \*\*112\*\*, 057203 \(2014\)](#).
- [47] M. Serbyn, Z. Papić, and D. A. Abanin, [Phys. Rev. Lett. \*\*111\*\*, 127201 \(2013\)](#)

## SUPPLEMENTARY MATERIAL

### A. Covariance matrix measurement in the stochastic series expansion

We calculate the covariance matrix  $\mathbf{C}$  within the stochastic series expansion approach. In the Hamiltonian Eqn.(1), the Ising term ( $S_i^z S_j^z$ ) and the magnetic terms ( $h_i S_i^z$ ) are the diagonal term  $\mathcal{O}^d$ , while the exchange term is the off-diagonal term  $\mathcal{O}^{od}$ . The covariance matrix is the product between two terms. In the stochastic series expansion (SSE) approach, we use different ways of measurement to calculate the quantum covariance matrix of the Hamiltonian [36, 42].

#### 1. $\mathcal{O}^d \mathcal{O}^d$ terms

As both of the terms belong to diagonal type operation, we can do direct measurement for every spin state along the non-empty operator string.

$$\langle \mathcal{O}^{d1} \mathcal{O}^{d2} \rangle = \left\langle \frac{1}{N_H} \sum_{p=1}^{N_H} \mathcal{O}_p^{d1} \mathcal{O}_p^{d2} \right\rangle \quad (4)$$

where  $N_H$  is the number of the non-empty in each measuring step,  $p$  is the slice index, and  $\langle \dots \rangle$  is the average of Monte Carlo steps. As the spin state only change during the off-diagonal operation, we can boost the efficiency by bookkeeping spins on most of the sites.

#### 2. $\mathcal{O}^{od} \mathcal{O}^{od}$ terms

Only the exchange-exchange term in  $\mathbf{C}$  belongs to this category. We cannot directly measure the off-diagonal term from the spin state. Instead, we use the number of appearance of the consecutive operators along the operator string to estimate its value.

$$\langle \mathcal{O}^{od1} \mathcal{O}^{od2} \rangle = \frac{1}{\beta^2} \langle (N_H - 1) N_{cons.}(\mathcal{O}^{od1}, \mathcal{O}^{od2}) \rangle \quad (5)$$

where  $N_{cons.}$  is the number of consecutive appearances of  $\mathcal{O}^{od1}$  and  $\mathcal{O}^{od2}$  in each Monte Carlo step.

#### 3. $\mathcal{O}^d \mathcal{O}^{od}$ terms

To calculate the combination of both diagonal and off-diagonal terms, we can combine both mentioned technique. At the occasion that  $\mathcal{O}^{od}$  appears, we measure the  $\mathcal{O}^d$  using direct measurement on the spin state.

$$\langle \mathcal{O}^{d1} \mathcal{O}^{od2} \rangle = \frac{1}{\beta} \left\langle \sum_{\mathcal{O}_p = \mathcal{O}^{od2}} \mathcal{O}_p^{d1} \right\rangle \quad (6)$$

where  $\mathcal{O}_p = \mathcal{O}^{od2}$  is the slice that the operator is off-diagonal.

### B. Benchmarking with Exact Diagonalisation

In order to establish the correctness of our quantum Monte Carlo (QMC) simulation, we have benchmarked our QMC program with the exact diagonalization (ED) technique on a 4 lattice. We show the comparison of the eigenstate-to-Hamiltonian construction (EHC) approach in Fig. 5. Though ED calculations may give an impression of giving higher critical values of the new disorder for the MBL transition; QMC simulations distinctly have the advantage of probing larger system sizes and thereby overcoming any finite size effects.

### C. Disorder from mapped Hamiltonian in real space

Using the eigenstate-to-Hamiltonian construction (EHC) formalism, we map the ground states of Eqn.(1), to obtain the target Hamiltonian in both the localized and delocalized regimes. The EHC mapping is successful in regimes, where the third smallest eigenvalue vanishes in the thermodynamic limit, so that we can obtain the mapped Hamiltonian with  $\tilde{h}$ . Unlike the initial disorder,  $h_i \in [-h, h]$ , which is random; the mapped disorder,  $\tilde{h}$ , shows local plateaus which are separated by large jumps in magnitude. In the localized regime, the magnitude of the jump in mapped disorder is large compared to the delocalized regime. The distribution of  $\tilde{h}$  in real space is shown in Fig.6 for representative  $h$  values in the delocalized and localized regimes respectively.

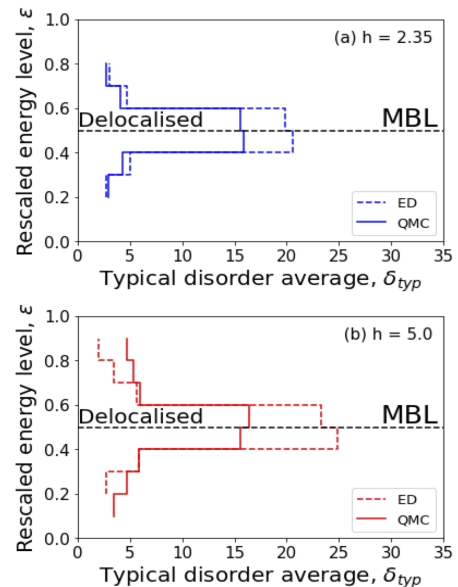


FIG. 5. Comparison of the MBL phase diagrams obtained from exact diagonalization (ED) and the quantum Monte Carlo (QMC) simulation on a  $4 \times 4$  square lattice, for (a)  $h = 2.35$  and (b)  $h = 5.0$ .

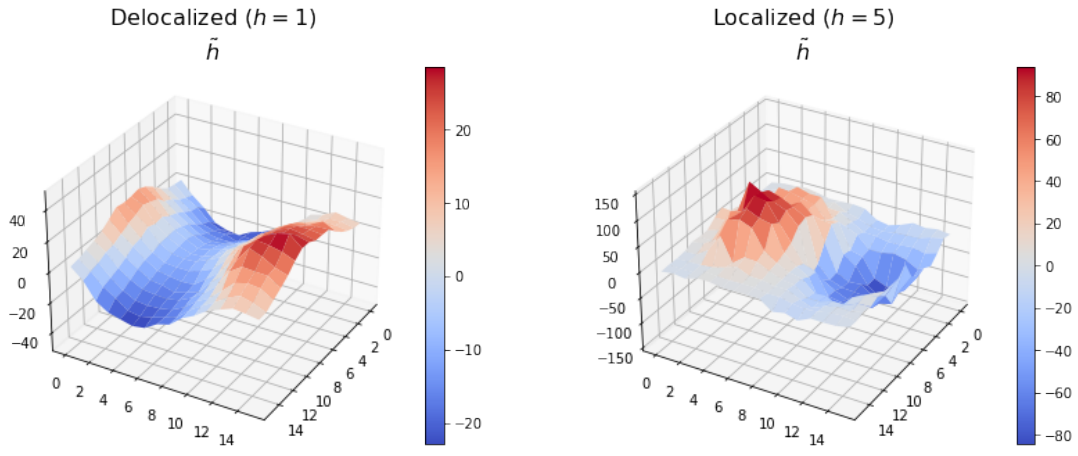


FIG. 6. Representative real space snapshots of the mapped disorder configuration obtained with the EHC formalism for (a)  $h = 1$  and (b)  $h = 5$  on a  $16 \times 16$  square lattice. Unlike the original random disorder,  $h_i \in [-h, h]$ ,  $\tilde{h}$  shows large jumps in magnitude in the localized regime, whereas the magnitude of variation in  $\tilde{h}$  is much smaller in the delocalized regime.